Asymptotic heat transfer model in thin liquid films

Marx Chhay, Denys Dutykh, Marguerite Gisclon, Christian Ruyer-Quil

Marx Chhay
LOCIE, Polytech Annecy–Chambéry, France

Denys Dutykh
CNRS, Université Savoie Mont Blanc, France

Marguerite Gisclon
CNRS, Université Savoie Mont Blanc, France

Christian Ruyer-Quil
LOCIE, Polytech Annecy–Chambéry, France

Asymptotic heat transfer model in thin liquid films

arXiv.org / HAL

Asymptotic heat transfer model in thin liquid films

Marx Chhay*, Denys Dutykh, Marguerite Gisclon,
and Christian Ruyer-Quil

Abstract. In this article, we present a modelling of heat transfer occuring through a liquid film flowing down a vertical wall. This model is formally derived thanks to asymptotic developpment, by considering the physical ratio of typical length scales of the study. A new Nusselt thermal solution is proposed, taking into account the hydrodynamic free surface variations and the contributions of the higher order terms in the asymptotic model are numerically pointed out. The comparisons are provided against the resolution of the full Fourier equations in a steady state frame.

Key words and phrases: Heat transfer; thin liquid film; asymptotic modelling; long waves

MSC: [2010]76D33 (primary), 76B25, 76B15 (secondary)

* Corresponding author.

Contents

1. Introduction

Falling liquid films have many significant applications in chemical engineering because of their reduced resistance to heat and mass transfers. They are generally encountered whenever the pressure drop is critical, *e.g.* in absorption machines, or whenever a low thermal driving force is required, for instance in the separation of multicomponent mixtures that are temperature-dependent. The dynamics of such flows have attracted a considerable interest as it presents a wavy regime organised around large-amplitude tear-drop like solitary waves whose interactions intensify transfers. This wavy regime is triggered by the classical Kapitza's long-wave instability. For this reason, the waves are long compared to the film thickness, they emerge at relatively long distances from the liquid inlet and they are slow to interact one with another. As a result, direct numerical simulations (DNSs) of such flows are hindered by the large domain that is necessary to account for their natural evolution, which explains that DNSs are generally restruicted to two-dimensional, *i.e.* spanwise independent, situations or to the construction of periodic waves.

Mathematical modeling offers a useful reduction of the numerical cost and a welcome framework for the undestanding of the disordered dynamics of such flows with the development of coherent-structure theories. Indeed, the large aspect ratio of the waves enables to introduce a small parameter ε, or film parameter, which compares the typical length of the wave to the thickness of the film. In this framework, the streamwise (x) and spanwise (y) coordinates as well as the time (t) are slow variables, *i.e.* $\partial_{x,y,t} \propto \varepsilon$, whereas the cross-stream coordinate is a fast variable ($\partial_z = \mathcal{O}(1)$). It is thus possible to eliminate the fast variable z and to obtain a reduced set of equations which describes the slow evolution of the film in a spatial domain whose dimension is reduced from 3D to 2D or from 2D to 1D if spanwise independent solutions are looked after. Following Kapitza's initial work [14], an important amount of work has been produced in order to derive such reduced set of equations or low-dimensional models (see for instance the review by [13]). Benney [2] thus showed that a series expansion of the flow variables with respect to the film parameter ε leads to a solution that is fully parametrised by the film thickness h and its gradients, the film dynamics being governed by a single evolution equation for h. Unfortunately, Benney's equation admits non-physical singularities in finite time at moderate Reynolds number [17] as a result of a too strict slaving of the velocity field to the free surface elevation. A cure to this shortcoming is offered within the Saint-Venant framework after averaging the primitive equation across the film depth. This idea dates back to the original work of Kapitza [14] and was successfully applied by Shkadov [26] who derived a set of two evolution equations for the local thickness h and the local flow rate q. Yet, consistent averaging of the primitive equations has been introduced only lately by Roberts [18] and Ruyer-Quil & Manneville [20] using different approaches.

Benney's original work has been extended in [11, 12] to deal with the conduction of heat across the film and the coupling of the hydrodynamics to the transfer offered by the dependence of surface tension on temperature (Marangoni effects). To account for moderate Reynolds number, Scheid *et al.* followed the weighted residual technique

initiated by Ruyer-Quil & Manneville [20] and derived several models of various accuracy [21, 24]. Though enabling to acurately decipher the complex interplay between the Kapitza hydrodynamic instability and the long-wave Marangoni thermocapillary instability [23], these models are only valid at relatively low values of the Peclet number. Indeed, as the Peclet number is raised, these models may predict unpysical values of the temperature. This behaviour is related to the onset of sharp temperature gradients at the free surface due to flow orientation in large-amplitude solitary waves. Though a cure to this limitation has been proposed by [27], available low-dimensional models still fail to capture correctly the temperature distribution at large Peclet number.

This article aims to perform a conservative formulation for heated falling film by applying a formal asymptotic development. The new formulation can be seen as a low-dimensional modelling of heated falling film flows following a derivation procedure that has been recently proposed by Vila and coworkers [3–5, 10]. This procedure, which will refer to thereinafter as the Saint-Venant consistent approach, is based on the classical Saint-Venant equations that are obtained by in-detph averaging of the primitive equations with a uniform weight. However, contrary to the Kapitza–Shkadov approach which assumes the velocity field to be strictly parabolic, Vila proposed a closure that is compatible with Benney's long-wave asymptotics and thus enables to accurately recover the threshold of the Kapitza instability.

The structure of the paper is as follows: in the next section, governing equations are recalled. Then some physical behaviour of the heated falling film are highlighted, using a basic modelisation, in order to introduce the dynamic of the system. In Section 3 the asymptotic model is derived. The computation is explicitely done until the first order terms. Thus, some numerical experiments in Section 4 finally illustrate in one hand the realistic behaviour of the model and, on the other hand, a comparison with an existing model in the literature is performed. Some discussion about the formal derivation conclude this work in Section 5.

2. Problem formulation

2.1. Governing equations

We consider an anisotherm liquid film flowing down a heated vertical plate. The flow is supposed to be two-dimensional in space, the x-axis corresponding to the streamwise direction and the z-axis to the cross-stream direction. The liquid domain is delimited by a vertical wall at $z = 0$ and the free surface boundary located at the height $z = h(x, t)$, such that the fluid layer is defined by

$$\Omega_t \;=\; \{(x, z) \;\in\; \mathbb{R}^2 \mid 0 \;<\; z \;<\; h(t, x)\}.$$

The sketch of the fluid domain is depicted in Figure 1.

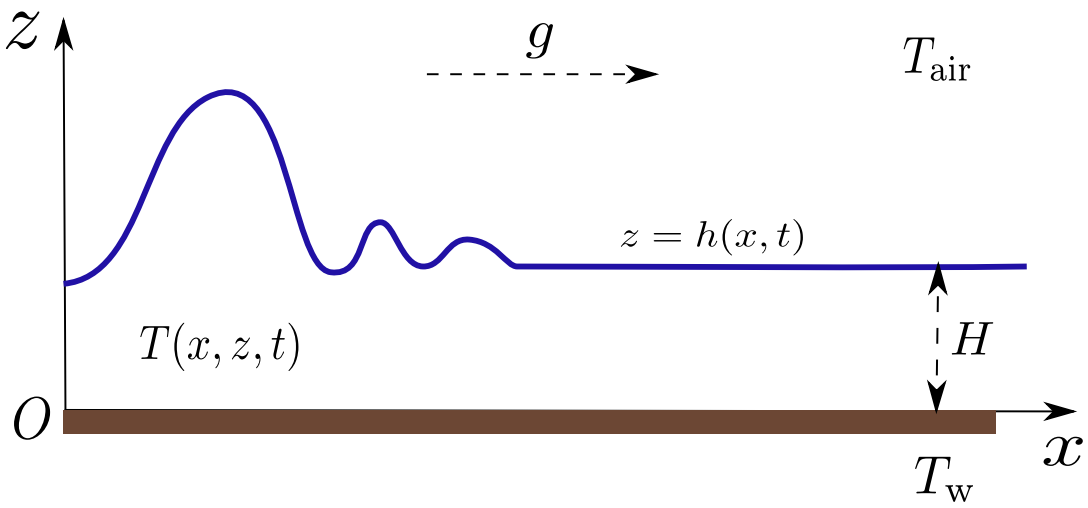

Figure 1. *Sketch of the physical fluid domain.*

The motion of the liquid is governed by the incompressible Navier–Stokes equations

$$\begin{aligned} \partial_t \boldsymbol{u} \;+\; (\boldsymbol{u}\cdot\boldsymbol{\nabla})\boldsymbol{u} \;&=\; -\frac{1}{\rho}\,\boldsymbol{\nabla} p \;+\; \nu\,\nabla^2\boldsymbol{u} \;+\; \mathbf{g}, \\ \boldsymbol{\nabla}\cdot\boldsymbol{u} \;&=\; 0, \end{aligned}$$

where $\boldsymbol{u} = (u, w)$, p and $\mathbf{g}$ represent the velocity and pressure fields and the gravity acceleration vector. The physical parameters ρ, ν correspond to the density and the kinematic viscosity. At the wall, a no-slip condition is imposed

$$\boldsymbol{u}|_{z=0} \;=\; 0,$$

while at the free surface, the kinematic condition governing the evolution of the fluid elevation reads

$$\partial_t h \;+\; u|_{z=h}\cdot\partial_x h \;=\; w|_{z=h}\,.$$

The continuity of the fluid stresses at the free surface gives

$$\begin{aligned} \partial_z u|_{z=h} \;+\; \partial_x w|_{z=h} \;&=\; -\,4\,\frac{\partial_x h}{1 \;-\; (\partial_x h)^2}\,\partial_z w|_{z=h} \\ p|_{z=h} \;+\; \kappa\,\frac{\partial^2_{xx} h}{[1 \;+\; (\partial_x h)^2]^{3/2}} \;&=\; -\,2\mu\,\frac{1 \;+\; (\partial_x h)^2}{1 \;-\; (\partial_x h)^2}\,\partial_x u|_{z=h}\,, \end{aligned}$$

where κ is the constant surface tension and $\mu = \rho\nu$ is the dynamic viscosity.

The heat transfer occuring through the liquid domain is modelled by the advection-diffusion Fourier equation

$$\partial_t T \;+\; \boldsymbol{u}\cdot\boldsymbol{\nabla} T \;=\; \alpha\,\nabla^2 T$$

where T corresponds to the temperature field and α is the thermal diffusion coefficient. A constant wall temperature is imposed

$$T|_{z=0} \;=\; T_{\text{wall}}\,.$$

Heat transfer at the free surface is modelled by a thermal exchange coefficient $\mathfrak{h}$ that is assumed to remain constant so that temperature field verifies the Newton's law of cooling at the free surface

$$-\lambda \left(\boldsymbol{\nabla} T \cdot \boldsymbol{n}\right)\big|_{z=h} \;=\; \mathfrak{h}\,\left[T\big|_{z=h} \;-\; T_{\text{air}}\right]$$

where λ and $\boldsymbol{n}$ denote the thermal conductivity and the unit exterior normal

$$\boldsymbol{n} \;=\; \frac{1}{\sqrt{1 \;+\; (\partial_x h)^2}} \begin{pmatrix} -\partial_x h \\ 1 \end{pmatrix}.$$

Notice that in the present study we do not consider strong coupling effects between the Hydrodynamics and the heat transfer. Namely, the temperature field T is advected by the fluid flow, but the temperature gradient $\boldsymbol{\nabla} T$ has no effect on the Hydrodynamics. It is certainly a simplification for the moment, but it will be released in our future investigations.

2.2. Scaled equations

The specific geometry of the falling film is caracterized by the typical length scales in both the streamwise direction and the cross-stream direction. The evolution of the hydrodynamic instabilities and the thermal diffusion process can also be described through these typical lengths.

Introducing the dimensionless quantities

- L : streamwise typical length scale,
- H : cross-stream typical length scale, The thin liquid depth is caracterized by the ratio $H \ll L$,
- $U_0 = gH^2/2\nu$: typical average velocity corresponding to hydrodynamic Nusselt solution,

and the following change of variables [5]:

$$t \;=\; \bar{t}\,\frac{L}{U_0}, \quad x \;=\; \bar{x}\,L, \quad z \;=\; \bar{z}\,H, \quad h \;=\; \bar{h}\,H, \quad u \;=\; \bar{u}\,U_0,$$

$$w \;=\; \bar{w}\,U_0 \frac{H}{L}, \quad p \;=\; \bar{p}\,\rho g H, \quad T \;=\; \bar{T}\,(T_{\text{wall}} \;-\; T_{\text{air}}) \;+\; T_{\text{air}}.$$

The dimensionless governing incompressilbe Fourier–Navier–Stokes equations finally read

$$\partial_t u \;+\; u\partial_x u \;+\; w\partial_z u \;+\; \frac{2}{\text{Re}}\,\partial_x p \;=\; \frac{2}{\varepsilon \text{Re}} \;+\; \frac{1}{\varepsilon \text{Re}}\,(\varepsilon^2 \partial^2_{xx} u \;+\; \partial^2_{zz} u), \tag{2.1}$$

$$\partial_t w \;+\; u\partial_x w \;+\; w\partial_z w \;+\; \frac{2}{\varepsilon^2 \text{Re}}\,\partial_z p \;=\; \frac{1}{\varepsilon \text{Re}}\,(\varepsilon^2 \partial^2_{xx} w \;+\; \partial^2_{zz} w), \tag{2.2}$$

$$\partial_x u \;+\; \partial_z w \;=\; 0, \tag{2.3}$$

$$\varepsilon\,\text{Pe}\,(\partial_t T \;+\; u\partial_x T \;+\; w\partial_z T) \;=\; \varepsilon^2 \partial^2_{xx} T \;+\; \partial^2_{zz} T \tag{2.4}$$

where $\varepsilon := \dfrac{H}{L}$ is the shallowness parameter. For convenience, the overbar notation for the dimensionless quantites have been dropped in the above equations. The no-slip boundary

condition at the wall

$$\boldsymbol{u}|_{z=0} \;=\; 0,$$

and the kinematic condition at the free surface

$$\partial_t h + u|_{z=h} \cdot \partial_x h \;=\; w|_{z=h}\,,$$

remain formally unmodified. The continuity conditions of the fluid stress across the free surface become

$$\begin{aligned} \partial_z u|_h \;+\; \varepsilon^2\, \partial_x w|_h \quad &=\quad -4\varepsilon^2\, \frac{\partial_x h}{1 \;-\; \varepsilon^2(\partial_x h)^2}\, \partial_z w|_h\,, \\ p|_h \;+\; \varepsilon^2\, \mathrm{We}\, \frac{\partial^2_{xx} h}{[1 \;+\; \varepsilon^2(\partial_x h)^2]^{3/2}} \quad &=\quad -\varepsilon\, \frac{1 \;+\; \varepsilon^2(\partial_x h)^2}{1 \;-\; \varepsilon^2(\partial_x h)^2}\, \partial_x u|_h\,. \end{aligned}$$

The dimensionless heat transfer between the heated liquid and the ambiant air becomes

$$\partial_z T|_h \;=\; -\sqrt{1 + (\varepsilon \partial_x h)^2}\; \mathrm{Bi}\; T|_h \;+\; \varepsilon^2\, \partial_x h\; \partial_x T|_h\,,$$

whereas the Dirichlet type boundary condition at the wall is

$$T|_{z=0} \;=\; 1.$$

Four dimensionless numbers characterize the problem at hand:

- the Reynolds number $\mathrm{Re} = U_0 H/\nu$,
- the Peclet number $\mathrm{Pe} = U_0 H/\alpha$,
- the Weber number $\mathrm{We} = \kappa/(\rho g H^2)$
- the Biot number $\mathrm{Bi} = \mathfrak{h} H/\lambda$.

This set of parameters will be usefully completed with the Kapitza number $\mathrm{Ka} = (l_c/l_\nu)^2 = \mathrm{We}\,(H/l_\nu)^2$ and $\widetilde{\mathrm{Bi}} = \mathfrak{h}\, l_\nu/\lambda = \mathrm{Bi}\, l_\nu/H$, where $l_c = \sqrt{\kappa/\rho g}$ is the capillary length, and $l_\nu = (\nu^2/g)^{1/3}$ is a viscous-gravity length [13]. The dimensionless groups Ka and $\widetilde{\mathrm{Bi}}$ are independent of the film thickness H and depend only on the fluid properties.

2.3. Fourier full 2D model

In order to illustrate numerically the heat transfer behaviour depending on relevant physical parameters, we present below some numerical simulations of the Fourier equation, the solution to the Navier–Stokes equation being approximated by the low-dimensional model that is presented below.

The numerical solution is looked after in a stationary rectangular domain thanks to the change of variables

$$\psi : (x, z, t) \;\mapsto\; \left(x, y = \frac{z}{h(x,t)}, t\right) \;\in\; [0, L] \times [0, 1] \times \mathbb{R}_+.$$

The transformed heat field $\theta = T \circ \psi^{-1}$ becomes a solution of

$$\varepsilon \mathrm{Pe}\; (\mathrm{D}_{t,h}\, \theta \;+\; \tilde{\boldsymbol{u}} \cdot \nabla_h \theta) \;=\; \Delta_h^2 \theta, \tag{2.5}$$

where the differential operators are given by

$$\begin{aligned}
\mathrm{D}_{t,h}\,\theta &= \partial_t\theta \;-\; \frac{y}{h}\,\partial_t h\,\partial_y\theta,\\
\nabla_h\theta &= \begin{pmatrix} \partial_x\theta \;-\; \dfrac{y}{h}\,\partial_x h\,\partial_y\theta \\ \dfrac{1}{h(x)}\,\partial_y\theta \end{pmatrix},\\
\Delta_h^2\theta &= \varepsilon^2\left[\partial_{xx}^2\theta \;-\; 2\frac{y}{h}\,\partial_x h\partial_{xy}^2\theta \;+\; \frac{y}{h}\left(\frac{2}{h}(\partial_x h)^2 \;-\; \partial_{xx}^2 h\right)\partial_y\theta\right]\\
&\quad + \left[\varepsilon^2\left(\frac{y}{h}\right)^2(\partial_x h)^2 \;+\; \frac{1}{h^2}\right]\partial_{yy}^2\theta
\end{aligned}$$

and $\tilde{\boldsymbol{u}} = (u - c, w)$ corresponds to the velocity vector field shifted by the wave celerity c.

The boundary condition at the wall remains

$$\theta|_{y=0} \;=\; 1,$$

and the Robin-type condition at the free surface becomes

$$\left(1 \;+\; (\varepsilon\,\partial_x h)^2\right)\,\partial_y\theta|_{y=1} \;-\; \varepsilon^2\,h\,\partial_x h\;\partial_x\theta|_{y=1} \;= -h\,\sqrt{1 \;+\; (\varepsilon\,\partial_x h)^2}\;\mathrm{Bi}\;\;\theta|_{y=1}\,.$$

The velocity field is computed using the parabolic approximation for the downstream component $u(x,z) = 3\left(z - \frac{1}{2}z^2\right)qh^{-1} - c$ with $q = \frac{1}{3} + c(h-1)$ and $c = 2.96$. The cross-stream velocity component $w(x,z)$ is computed such that the incompressibility is verified.

The numerical results for the steady temperature profile are obtained using an implicit second order scheme. The isothermal lines plotted in Figure 2 have been computed from Equation (2.5) for an analogous configuration as is [28]. The solitary wave profile and the velocity field under the wave were obtained from Vila's model [4]. The Reynolds number is fixed at $\mathrm{Re} = 7.5$, $\mathrm{Ka} = 3000$ for various fluid properties (Pr and $\mathrm{Bi} = (2\mathrm{Re})^{1/3}\widetilde{\mathrm{Bi}}$).

When no heat transfer is allowed between the liquid film and the surrounding air, the falling film reaches the uniform temperature given by the heated wall ($\mathrm{Bi} \to 0$). When heat exchange between the two fluids phases is maximal ($\mathrm{Bi} \to \infty$), the liquid film behaves as a conductive medium between the heated wall and the colder air.

The temperature follows a linear distribution across a flat film (Nusselt solution). However, as soon as hydrodynamic instabilities occur, a recirculation zone within large-amplitude waves may appear when the fields are described from the wave moving frame. The heat transfer through the liquid film is locally far from being linear. This corresponds to the physical mechanism of heat enhencement, as used in engineering process. In case of vertical falling film, Benjamin [1] has shown the appearance of such inertial hydrodynamic instabilities. Therefore, when considering the vertical configuration of anisotherm falling film, the intensification of heat transfer by the hydrodynamic instabilities must be taken into account. The hypothesis of flat falling film does not stand anymore.

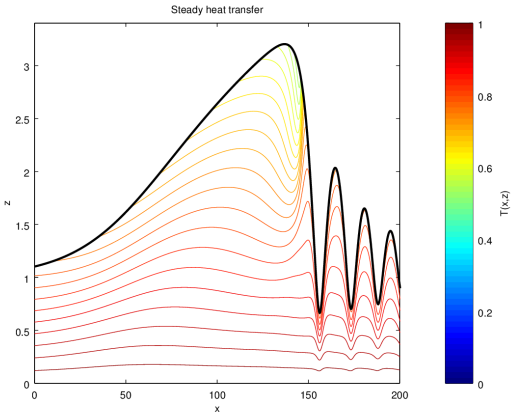

(a) $\widetilde{\mathrm{Bi}} = 0.1, \mathrm{Pr} = 7$

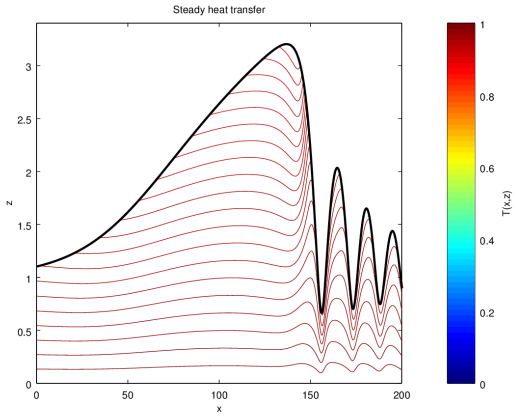

(b) $\mathrm{Pr} = 1, \widetilde{\mathrm{Bi}} = 0.01$

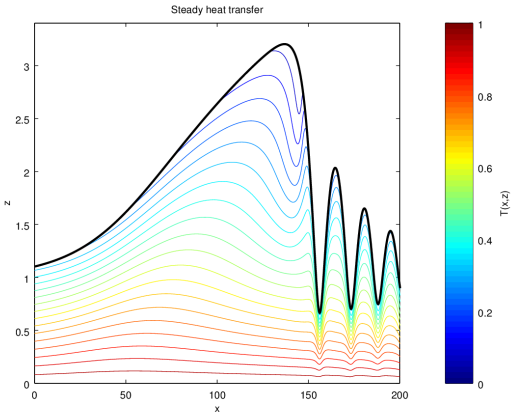

(c) $\widetilde{\mathrm{Bi}} = 1, \mathrm{Pr} = 7$

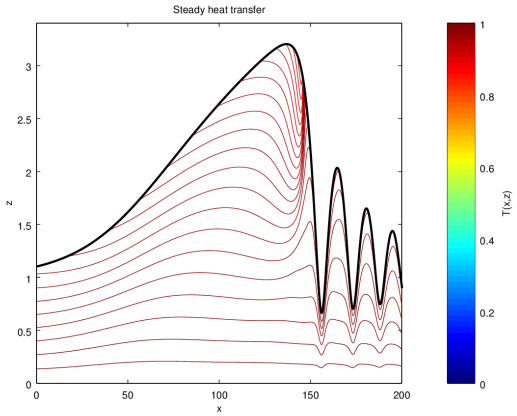

(d) $\mathrm{Pr} = 7, \widetilde{\mathrm{Bi}} = 0.01$

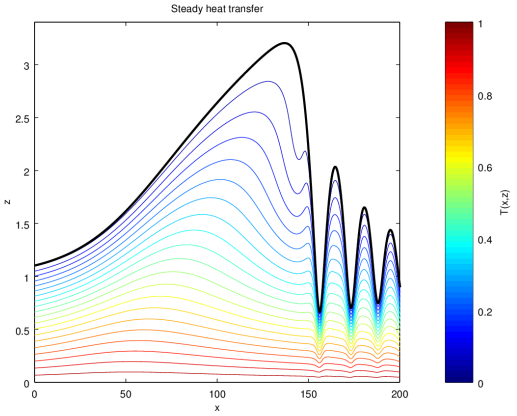

(e) $\widetilde{\mathrm{Bi}} = 10, \mathrm{Pr} = 7$

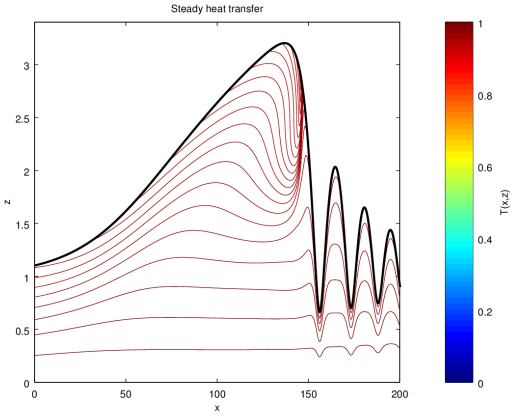

(f) $\mathrm{Pr} = 30, \widetilde{\mathrm{Bi}} = 0.01$

Figure 2. On the left column: *Isotherms in the intertial frame for different* $\widetilde{\mathrm{Bi}}$ *numbers and* $\mathrm{Pr} = 7$. *As expected, the temperature field is more uniform when no heat transfer is allowed with the free surface.* On the right column: *Isotherms in the intertial frame for different* Pr *number. The recirculation zone occurs as the advective part becomes dominant against the diffusive process. Heat flux becomes locally strongly non linear.* $\widetilde{\mathrm{Bi}} = 0.01$.

3. Asymptotic model

In what follows, we present the derivation of a system of averaged equations for the mass, momentum and heat balances (2.1)–(2.4) following the classical Saint-Venant approach. Consistency with the long-wave asymptotic expansion of the flow variables with respect to the parameter ε is guaranteed by computing the higher order corrections to the thermal Nusselt solution, corresponding to the leading order term of the asymptotic developpement for the temperature field.

3.1. Thermal Nusselt solution

Consider a formal expansion for the temperature field with respect to the small order parameter ε

$$T \;=\; T^{(0)} \;+\; \varepsilon T^{(1)} \;+\; \varepsilon^2 T^{(2)} \;+\; \cdots \;+\; \varepsilon^n T^{(n)} \;+\; \mathcal{O}(\varepsilon^{n+1}). \tag{3.1}$$

By substituting the development (3.1) into the dimensionless Fourier equation (2.4) and by taking the limit $\varepsilon \to 0$, we obtain the explicit temperature profile for the leading order term $T^{(0)}$:

Proposition 1. *The main order term $T^{(0)}$, called the thermal Nusselt solution, is given by*

$$T^{(0)}(x,z,t) \;=\; 1 \;-\; A(x,t)\,z \quad \text{with} \quad A(x,t) \;=\; \frac{\sqrt{1 \;+\; (\varepsilon\partial_x h)^2}\ \mathrm{Bi}}{1 + h\sqrt{1 + (\varepsilon\partial_x h)^2}\ \mathrm{Bi}}. \tag{3.2}$$

We can remark that the Nusselt thermal gradient A is function of h and its first derivative.

Proof. The substitution of the formal expansion (3.1) into the dimensionless Fourier equation yields

$$\partial^2_{zz} T^{(0)} \;=\; 0,$$

when ε tends to 0. Taking into account the associated boundary conditions

$$T^{(0)}\big|_{z=0} \;=\; 1\,, \qquad \partial_z T^{(0)}\big|_{z=h} \;=\; -\sqrt{1 \;+\; (\varepsilon\partial_x h)^2}\ \mathrm{Bi}\ T^{(0)}\big|_{z=h}$$

the resolution of the second order differential equation gives the expected expression for the main order temperature profile. □

Although its computation is straightforward, the expression of the thermal Nusselt solution differs from the linear temperature profile found in the literature [7, 22]. The thermal gradient A in Proposition 1 involves the liquid film height h depending on the x. Thus the proposed thermal Nusselt solution traduces with more accuracy the influence of the hydrodynamic instabilites than as if its linear factor would just have been constant along the downslope direction. It is worth to point out that, even when $\varepsilon \to 0$, travelling waves may appear as solutions of the Shallow Water model. Thus, even in this limit case ($\varepsilon = 0$), the falling film profile may vary along the downslope direction and it is expected for the thermal Nusselt solution to traduce also this behaviour.

Remark 1. *The average Nusselt solution* $\overline{T}^{(0)} = \dfrac{1}{h}\displaystyle\int_0^h T^{(0)}\,\mathrm{d}z$ *is consistent with the limit cases of heat transfer. Indeed out of the instability neighborhood, the uniform temperature profile is reached (adiabatic case:* $\mathrm{Bi} \to 0$, $\overline{T}^{(0)} \to 1$*) and whereas when no resistance to the transfer at the free surface happens,* $\mathrm{Bi} \to \infty$*, the linear heat profile occurs, yielding* $\overline{T}^{(0)} \to \dfrac{1}{2}$.

3.2. Formal derivation of the asymptotic heat transfer model

In the following, we set

$$\mathcal{B} \;=\; \sqrt{1 \;+\; (\varepsilon \partial_x h)^2}\;\mathrm{Bi} \;=\; \mathcal{O}(\mathrm{Bi}), \tag{3.3}$$

then

$$A \;=\; \frac{\mathcal{B}}{1 \;+\; h\,\mathcal{B}}. \tag{3.4}$$

We introduce the averaged temperature

$$\overline{T} \;=\; \frac{1}{h}\int_0^h T\,\mathrm{d}z.$$

Since $T \;=\; T^{(0)} \;+\; \varepsilon T^{(1)} + \;\mathcal{O}(\varepsilon^2)$ with $T^{(0)} \;=\; 1 \;-\; A\,z$ we introduce

$$\theta \;:=\; 1 \;-\; \overline{T} \;=\; \frac{1}{2}\,A\,h \;-\; \frac{\varepsilon}{h}\int_0^h T^{(1)}\,\mathrm{d}z \;+\; \mathcal{O}(\varepsilon^2). \tag{3.5}$$

We derive formally an evolution equation related to the mean temperature field following the consistent Saint-Venant approach. The main result is then

Proposition 2 (Asymptotic heat transfer model)**.** *The conservative formulation of the model for the shifted mean temperature field* θ *reads*

$$\partial_t(h\theta) \;+\; \partial_x(vh\theta) \;=\; \frac{6N}{5\varepsilon\mathrm{Pe}} \;-\; \frac{1}{75}\,(8 \;-\; 9h\mathcal{B})\,\partial_x\Big(\frac{h^4\mathcal{B}}{1+h\mathcal{B}}\Big) \;+\; \partial_x D \;+\; \mathcal{O}(\varepsilon) \tag{3.6}$$

with

$$D \;=\; \frac{27}{50\mathcal{B}^3}\left(-\ln|1+h\mathcal{B}| \;+\; h\mathcal{B} \;-\; \frac{(h\mathcal{B})^2}{2} \;+\; \frac{(h\mathcal{B})^3}{3} \;-\; \frac{7(h\mathcal{B})^4}{36}\right).$$

The term N *stands for the main order part, yielding the thermal Nusselt solution*

$$N \;=\; -\mathcal{B} \;+\; \frac{2(1+h\mathcal{B})}{h}\,\theta.$$

In order to compute the asymptotic model, we first compute some integrals occuring in higher terms of the formal development. The longitudinal velocity component u expands in the form

$$u(t,x,z) \;=\; u^{(0)}(t,x,z) \;+\; \mathcal{O}(\varepsilon) \;=\; 2h(t,x)\,z \;-\; z^2 \;+\; \mathcal{O}(\varepsilon).$$

The transverse component velocity w is determined using the free divergence condition and the no slip condition $w(x,0)=0$. More precisely, we find

$$w(t,x,z) \;=\; -\int_0^z \partial_x u(t,x,y)\,\mathrm{d}y \;=\; -z^2\,\partial_x h(t,x) \;+\; \mathcal{O}(\varepsilon) \;=\; w^{(0)}(t,x,z) \;+\; \mathcal{O}(\varepsilon).$$

Lemma 1. *The average quantity of the unsteady advective term, at the main order, is given thanks to the computation of the following integral*

$$I_3(y) \;=\; \int_y^h \left(\partial_t T^{(0)} \;+\; u^{(0)}\partial_x T^{(0)} \;+\; w^{(0)}\partial_z T^{(0)}\right)\,\mathrm{d}\xi$$

that reads in terms of the Nusselt thermal gradient A

$$I_3(y) \;=\; \frac{1}{2}(h^2-y^2)\partial_t A \;+\; \left(\frac{5}{12}h^4 - \frac{2}{3}y^3\,h + \frac{1}{4}y^4\right)\partial_x A \;-\; \frac{1}{3}(h^3-y^3)A\partial_x h.$$

We introduce

$$\begin{aligned} I_2(z) \;&=\; \int_0^z I_3(y)\,\mathrm{d}y \\ &=\; \frac{1}{2}\left(h^2 z - \frac{z^3}{3}\right)\partial_t A \;+\; \left(\frac{5}{12}\,h^4 z - \frac{1}{6}\,h z^4 + \frac{1}{20}\,z^5\right)\partial_x A \\ &\quad -\; \frac{A}{3}\left(h^3 z - \frac{1}{4}z^4\right)\partial_x h \end{aligned}$$

then

$$\begin{aligned} \int_0^h\int_0^z I_3(y)\,\mathrm{d}y\,\mathrm{d}z \;&=\; \int_0^h I_2(z)\,\mathrm{d}z \\ &=\; \frac{5}{24}\,h^4\,\partial_t A \;+\; \frac{11}{60}\,h^6\,\partial_x A \;-\; \frac{3}{2}\,h^5\,\partial_x h\,A. \end{aligned}$$

Proof. A direct substitution of $T^{(0)}(x,z,t) = 1 - A(x,t)\,z$ into the integral yields

$$I_3(y) \;=\; \int_y^h \left(\xi\,\partial_t A \;+\; \xi\,u^{(0)}\,\partial_x A \;+\; w^{(0)}\,A\right)\,\mathrm{d}\xi$$

Taking $u^{(0)} = 2zh - z^2$ and $w^{(0)} = -z^2\,\partial_x h$, we obtain

$$\begin{aligned} I_3(y) \;&=\; \int_y^h \left(\xi\partial_t A \;+\; 2h\xi^2\partial_x A \;-\; \xi^3\partial_x A \;-\; (\partial_x h)\xi^2 A\right)\,\mathrm{d}\xi \\ &=\; \frac{1}{2}\,(h^2-y^2)\partial_t A \;+\; \frac{2h}{3}(h^3-y^3)\partial_x A \;-\; \frac{1}{4}\,(h^4-y^4)\partial_x A \\ &\quad -\; \frac{1}{3}\,\partial_x h\,(h^3-y^3)A, \end{aligned}$$

that gives the result for I_3. The computations related to I_2 are straightforward. □

We recall that the formal development of the temperature field following the order parameter ε is:

$$T \;=\; 1 \;-\; A\,z \;+\; \varepsilon T^{(1)} \;+\; \mathcal{O}(\varepsilon^2)$$

with the ansatz for A given by (3.2) then we have the following result

Proposition 3 ($T^{(1)}$ computation). *The second order of the formal development of the temperature field is given by*

$$\begin{aligned} T^{(1)}(x,z,t) \;=\; & z\,\frac{\mathrm{Pe}\,\mathcal{B}}{1+h\mathcal{B}}\left(\frac{1}{3}\,h^3\partial_t A \;+\; \frac{3}{10}\,h^5\partial_x A \;-\; \frac{1}{4}\,Ah^4\partial_x h\right) \\ & -\mathrm{Pe}\left(\frac{1}{2}\,(h^2 z-\frac{z^3}{3})\,\partial_t A \;+\; (\frac{5}{12}h^4 z-\frac{1}{6}hz^4+\frac{1}{20}z^5)\,\partial_x A\right. \\ & \left.-\frac{A}{3}(h^3 z-\frac{1}{4}\,z^4)\,\partial_x h\right). \end{aligned}$$

Proof. The first order terms in $\mathcal{O}(\varepsilon)$ occuring in the dimensionless Fourier equation and the boundary condition at the free surface yield

$$T^{(1)}(z) \;=\; z\;\partial_z T^{(1)}\big|_{z=h} \;-\; \mathrm{Pe}\,I_2(z) \quad\text{and}\quad \partial_z T^{(1)}\big|_{z=h} \;=\; -\mathcal{B}\;T^{(1)}\big|_{z=h}\,,$$

then

$$T^{(1)}(z) \;=\; -z\,\mathcal{B}\;T^{(1)}\big|_{z=h} \;-\; \mathrm{Pe}\,I_2(z)$$

but

$$\begin{aligned} T^{(1)}(h) \;&=\; \frac{-\mathrm{Pe}}{1+h\mathcal{B}}\;I_2(h) \\ &=\; \frac{-\mathrm{Pe}}{1+h\mathcal{B}}\left(\frac{1}{3}\,h^3\,\partial_t A \;+\; \frac{3}{10}\,h^5\,\partial_x A \;-\; \frac{1}{4}\,Ah^4\,\partial_x h\right). \end{aligned}$$

Proposition is obtained by re-injecting this expression into the equation on $T^{(1)}$. □

Now we can establish the Asymptotic heat transfer model:

Proposition 2. We integrate the equation on the temperature with respect to z

$$\varepsilon\,\mathrm{Pe}\int_0^h (\partial_t T \;+\; u\partial_x T \;+\; w\partial_z T)\;\mathrm{d}z \;=\; \int_0^h \left(\varepsilon^2\,\partial^2_{xx}T \;+\; \partial^2_{zz}T\right)\;\mathrm{d}z$$

then

$$\varepsilon\,\mathrm{Pe}\left(\partial_t\int_0^h T\,\mathrm{d}z \;+\; \partial_x\int_0^h (uT)\,\mathrm{d}z\right) \;=\; -\mathcal{B}\;T|_{z=h} \;-\; \partial_z T|_{z=0} \;+\; \mathcal{O}(\varepsilon^2),$$

which is obtained thanks to

$$\begin{aligned} \partial_t\int_0^h T\;\mathrm{d}z \;&=\; T|_{z=h}\,\partial_t h \;+\; \int_0^h \partial_t T\;\mathrm{d}z \\ \text{and}\quad \partial_x\int_0^h uT\;\mathrm{d}z \;&=\; (uT)|_{z=h}\,\partial_x h \;+\; \int_0^h \partial_x(uT)\;\mathrm{d}z \end{aligned}$$

and to the boundary condition:

$$-\,\partial_z T|_{z=h} \;=\; \mathcal{B}\;T|_{z=h} \;+\; \mathcal{O}(\varepsilon^2) \qquad \partial_t h + u|_{z=h}\,\partial_x h \;=\; \mathcal{O}(\varepsilon^2).$$

Thanks to Ansatz (3.2) we can write

$$A \;=\; \frac{2}{h}\,(1-\overline{T}) \;+\; \frac{2\varepsilon}{h^2}\int_0^h T^{(1)}\,\mathrm{d}z \;+\; \mathcal{O}(\varepsilon^2)$$

and

$$\begin{aligned}
\int_0^h u\,T\,\mathrm{d}z \;&=\; \int_0^h u^{(0)}\,T^{(0)}\,\mathrm{d}z \;+\; \mathcal{O}(\varepsilon)\\
&=\; \int_0^h (2hz \;-\; z^2)(1 \;-\; Az)\,\mathrm{d}z \;+\; \mathcal{O}(\varepsilon)\\
&=\; \int_0^h (2hz \;-\; z^2)(1 \;+\; \frac{2}{h}\,(\overline{T} \;-\; 1))\,\mathrm{d}z \;+\; \mathcal{O}(\varepsilon)\\
&=\; -\frac{1}{6}\,h^3 \;+\; \frac{5}{6}\,\overline{T}\,h^3 \;+\; \mathcal{O}(\varepsilon).
\end{aligned}$$

The integrated equation becomes

$$\varepsilon\,\mathrm{Pe}\left(\partial_t(h\overline{T}) \;+\; \partial_x\Big(\frac{5}{6}\,\overline{T}\,h^3 \;-\; \frac{1}{6}\,h^3\Big)\right) \;=\; -\mathcal{B}\;T\big|_{z=h} \;-\; \partial_z T\big|_{z=0} \;+\; \mathcal{O}(\varepsilon^2),$$

with

$$\begin{aligned}
T\big|_{z=h} \;&=\; T^{(0)}\big|_{z=h} \;+\; \varepsilon\,T^{(1)}\big|_{z=h} \;+\; \mathcal{O}(\varepsilon^2)\\
&=\; 1 \;+\; Ah \;+\; \varepsilon\,T^{(1)}\big|_{z=h} \;+\; \mathcal{O}(\varepsilon^2)\\
&=\; 2\overline{T} \;-\; 1 \;-\; \frac{2\varepsilon}{h}\int_0^h \big[T^{(1)} \;+\; \varepsilon\,T^{(1)}\big|_{z=h}\big]\,\mathrm{d}z \;+\; \mathcal{O}(\varepsilon^2).
\end{aligned}$$

It remains to compute $\partial_z T\big|_{z=0}$ in the above equation:

$$\begin{aligned}
\partial_z T\big|_{z=0} \;&=\; \partial_z(T^{(0)} \;+\; \varepsilon T^{(1)})\big|_{z=0} \;+\; \mathcal{O}(\varepsilon^2)\\
&=\; -A \;+\; \varepsilon\;\partial_z T^{(1)}\big|_{z=0} \;+\; \mathcal{O}(\varepsilon^2)\\
&=\; \frac{2}{h}\,(\overline{T} \;-\; 1) \;-\; \frac{2\varepsilon}{h^2}\int_0^h T^{(1)}\,\mathrm{d}z \;+\; \varepsilon\;\partial_z T^{(1)}\big|_{z=0} \;+\; \mathcal{O}(\varepsilon^2).
\end{aligned}$$

Then the integrated equation reads

$$\mathrm{Pe}\left(\partial_t(h\overline{T}) \;+\; \partial_x\Big(\frac{5}{6}\,\overline{T}\,h^3 \;-\; \frac{1}{6}\,h^3\Big)\right) \;=\; \frac{1}{\varepsilon}N \;+\; S \;+\; \mathcal{O}(\varepsilon),$$

with

$$S \;=\; -\mathcal{B}\;T^{(1)}\big|_{z=h} \;-\; \partial_z T^{(1)}\big|_{z=0} \;+\; \frac{2}{h^2}\,(1+h\mathcal{B})\int_0^h T^{(1)}\,\mathrm{d}z.$$

Surprisingly the first two terms of S vanishe with the left hand side of the integrated Fourier equation. Indeed, from the above computations, we get

$$\begin{aligned} -\mathcal{B}\, T^{(1)}\big|_{z=h} \;-\; \partial_z T^{(1)}\big|_{z=0} &= \mathrm{Pe}\; I_3(0) \\ &= \mathrm{Pe}\int_0^h \left(\partial_t T^{(0)} \;+\; u^{(0)}\partial_x T^{(0)} \;+\; w^{(0)}\partial_z T^{(0)}\right) \mathrm{d}z \\ &= \mathrm{Pe}\left[\partial_t(h\overline{T}) \;-\; \frac{1}{6}\,\partial_x h^3 \;+\; \frac{5}{6}\,\partial_x(h^3\overline{T})\right] \end{aligned}$$

Finally the integrated equation reduces to

$$\frac{1}{\varepsilon}\,N \;+\; S_1 \;=\; \mathcal{O}(\varepsilon), \tag{3.8}$$

with

$$N \;=\; \frac{2(1 \;+\; h\mathcal{B})}{h}\left(\frac{1 \;+\; \frac{1}{2}h\mathcal{B}}{1 \;+\; h\mathcal{B}} \;-\; \overline{T}\right) \quad \text{and} \quad S_1 \;=\; \frac{2}{h^2}(1+h\mathcal{B})\int_0^h T^{(1)}\,\mathrm{d}z,$$

where $\displaystyle\int_0^h T^{(1)}\,\mathrm{d}z$ can be explicitely computed thanks to its expression given in Proposition 3 and using that

$$A \;=\; \frac{2}{h}\,(1-\overline{T}) \;+\; \mathcal{O}(\varepsilon) \;=\; \frac{2}{h}\,\theta \;+\; \mathcal{O}(\varepsilon) \quad \text{and} \quad \partial_t h \;=\; -2h^2\,\partial_x h \;+\; \mathcal{O}(\varepsilon).$$

We finally get

$$\begin{aligned} \frac{1}{\mathrm{Pe}}S_1 \;=\;& h\mathcal{B}\left(\frac{1}{6}\,\partial_t(h\overline{T}) \;+\; \frac{2}{15}\,\partial_x(h^3\overline{T}) \;-\; \frac{1}{30}\,\overline{T}h^2\partial_x h \;-\; \frac{1}{30}\,\partial_x h^3\right) \\ &-\left(\frac{5}{6}\,\partial_t(h\overline{T}) \;-\; \frac{11}{15}\,\partial_x(h^3\overline{T}) \;-\; \frac{1}{5}\,\overline{T}h^2\partial_x h \;-\; \frac{1}{9}\,\partial_x h^3\right) \;+\; \mathcal{O}(\varepsilon). \end{aligned}$$

Substituting it in Equation (3.8), the final depth-averaged heat equation reads

$$5(5+h\mathcal{B})\,\partial_t(h\overline{T}) \;+\; 4\Big(\frac{11}{2} \;+\; h\mathcal{B}\Big)\partial_x(h^3\overline{T}) \;=\; \frac{30}{\varepsilon\mathrm{Pe}}\,N \;+\; D \;+\; \mathcal{O}(\varepsilon) \tag{3.9}$$

with

$$D \;=\; \left(\frac{10}{3} \;+\; h\mathcal{B}\right)\partial_x h^3 \;+\; (6 \;-\; h\mathcal{B})\,h^2\,\overline{T}\,\partial_x h.$$

In order to obtain a conservative form for a quantity related to the mean temperature, it is necessary to remove all the terms in factor with $h\mathcal{B}$ in Equation (3.9). For this purpose, we recall that the shifted mean temperature field θ is given by Equation (3.5) with A defined in (3.4) then

$$\begin{aligned} \theta \;&=\; \frac{h}{2}\,A \;+\; \mathcal{O}(\varepsilon) \\ &=\; \frac{h}{2}\,\frac{\mathcal{B}}{1 \;+\; h\mathcal{B}} \;+\; \mathcal{O}(\varepsilon) \end{aligned} \tag{3.10}$$

such that

$$h\,\mathcal{B} \;=\; \frac{2\theta}{1 \;-\; 2\theta} \;+\; \mathcal{O}(\varepsilon).$$

Thus, in one hand the thermal Nusselt solution finally reads

$$N \;=\; -\mathcal{B} \;+\; \frac{2(1 \;+\; h\mathcal{B})}{h}\,\theta$$

and on the other hand, Equation (3.9) becomes

$$\partial_t(h\theta) \;+\; \partial_x(hv\theta) \;=\; \frac{6}{5\varepsilon\mathrm{Pe}}\,N \;+\; D' \;+\; \mathcal{O}(\varepsilon), \tag{3.11}$$

with

$$D' \;=\; -\frac{2}{25}\,(4 + 3h\mathcal{B})\,\partial_x(hv\theta) \;+\; \frac{9}{50}\,(\,2 + 3h\mathcal{B}\,)\,v\,\theta\,\partial_x h \;+\; \frac{2}{5}\,\theta^2\,\partial_x(hv)$$

The term D' appears in the right hand side of Equation (3.11) can be expressed in terms of the variable h only thanks to the substitution $v = \frac{2}{3}h^2$ and Equation (3.10). Thus, after some straitforward algebraic computations, one gets the asymptotic heat transfer model (3.6). □

Thus, finally the full anisothermal hydrodynamic model reads in vectorial form

$$\partial_t\mathcal{U} \;+\; \partial_x\mathcal{F} \;=\; \frac{1}{\varepsilon}\,\mathcal{N} \;+\; \mathcal{S} \tag{3.12}$$

with

$$U \;=\; \begin{pmatrix} h \\ hv \\ h\theta \end{pmatrix}, \qquad \mathcal{F} \;=\; \begin{pmatrix} hv \\ hv^2 \;+\; \dfrac{8}{225}\,h^5 \\ h\theta v \end{pmatrix},$$

$$\mathcal{N} \;=\; \begin{pmatrix} 0 \\ \dfrac{1}{\mathrm{Re}}\Big(2h \;-\; \dfrac{3v}{h}\Big) \\ \dfrac{6}{5\mathrm{Pe}}\Big(\mathcal{B} \;-\; \dfrac{2(1 + h\mathcal{B})}{h}\,\theta\Big) \end{pmatrix}, \qquad \mathcal{S} \;=\; \begin{pmatrix} 0 \\ \mathrm{We}\,h\,h_{xxx} \\ Q(h) \end{pmatrix},$$

where

$$Q(h) \;=\; -\frac{1}{75}\,(8 \;-\; 9h\mathcal{B})\,\partial_x\left(\frac{h^4\mathcal{B}}{1 \;+\; h\mathcal{B}}\right) \;+\; \frac{27}{50\mathcal{B}^3}\,\partial_x\Big[-\ln|1 + h\mathcal{B}| \;+\; h\mathcal{B} \;-\; \frac{(h\mathcal{B})^2}{2} \;+\; \frac{(h\mathcal{B})^3}{3} \;-\; \frac{7(h\mathcal{B})^4}{36}\Big].$$

The third component of this vectorial equation, corresponding to the temperature field, can be recast such that $\mathcal{S}_3 = 0$ and

$$\mathcal{F}_3 = h\theta v + \frac{1}{600\mathcal{B}^3}\Big[\frac{136}{1+h\mathcal{B}} + 396 - \ln|1+h\mathcal{B}| - 260h\mathcal{B} + 62(h\mathcal{B})^2 + 4(h\mathcal{B})^3 + 9(h\mathcal{B})^4\Big].$$

In formulas above ($\mathcal{S}_3$, $\mathcal{F}_3$) the index denotes the component number in the corresponding vector ($\mathcal{S}$, $\mathcal{F}$).

The obtained system of equations must be contrasted with the non-conservative system corresponding to the averaged energy balance derived in [27] following the weighted residual approach introduced by [21]:

$$\partial_t\varphi + \frac{27}{20}\,v\,\partial_x\varphi - \frac{7}{40}\frac{1-\varphi}{h}\,\partial_x(vh) = \frac{3}{h^2}\big[1 - \big(1 + \mathcal{B}h\big)\varphi\big] \tag{3.13}$$

where φ refers to the free surface temperature of the flow, *i.e.*

$$\varphi = 1 - 2\theta + \mathcal{O}(\varepsilon).$$

The two descriptions of the energy balance are consistent at $\mathcal{O}(\varepsilon)$ and thereofre shall yield the similar results as long as the long-wave expansion strictly holds. Yet, Equation (3.13) has the disadvantage not to admit a conservative form.

4. Numerical illustrations

In this section, we study first the time-space behaviour of the asymptotic model for the average temperature field $\overline{T}$. A hyperbolic scheme is implemented in order to take the full advantage of the conservative formulation of Model (3.12). A second numerical test is performed, illustrating the global behaviour of the model in function of the physical parameters Re, Bi, Pe. The solutions representation corresponds to the dynamical system point of view, and is realized thanks to the `AUTO07p` software [8]. Notice that for the sake of simplicity in all computations below we adopt the assumption (3.3).

4.1. Unsteady simulations

The hyperbolicity of System (3.12) can be easily checked by computing the eigenvalues of the advective flux $\mathcal{F}(\mathcal{U})$ Jacobian matrix:

$$\mathcal{A} = \frac{\partial\mathcal{F}}{\partial\mathcal{U}} = \begin{pmatrix} 0 & 1 & 0 \\ -v^2 + \dfrac{8}{45}h^4 & 2v & 0 \\ \theta u & \theta & u \end{pmatrix}.$$

The eigenvalues of the matrix $\mathcal{A}$ can be readily computed. Indeed, after simple algebraic computations we obtain three distinct eigenvalues provided $h > 0$:

$$\lambda_0 \;=\; v, \qquad \lambda_\pm \;=\; v \;\pm\; \frac{2}{15}\sqrt{10}h^2.$$

Thus, we just showed the hyperbolicity of System 3.12. The eigenstructure of the advective flux $\mathcal{F}(\mathcal{U})$ will be used below to solve numerically the System 3.12 of balance laws with the widely-known Rusanov scheme. In order to solve numerical the conservative part of thermal Saint-Venant equations we employ the standard finite volume discretization [9] along with the Rusanov scheme [19]. The dispersive (*i.e.* the capillary force) and other non-conservative terms were discretized using the central finite differences. Good numerical properties of this combination were demonstrated recently in [15]. For the time discretization we use the variable order Adams–Bashforth–Moulton predictor-corrector solver, which is implemented in Matlab in `ode113` routine [25]. The absolute and relative tolerances were both set to 10^{-6} in simulations shown below.

Starting with an arbitrary reasonable initial condition

$$h_0(x) \;=\; 1 \;+\; \frac{1}{2}\,\sin^2\!\Big(\frac{25\pi x L}{10000}\Big),$$

and $T_0 = 0.7$ and using periodic boundary conditions, the solution reaches its hydrodynamical steady-state at around $t = 17.5$, whereas the steady state thermal regime takes place a little bit after at around $t = 20$. The parameters are $\mathcal{B} = 1$, $\mathrm{Re} = 1$, $\mathrm{Pe} = 10$. The minimal value of T is stabilized very quickly at around $T_{\min} = 5.2$: the fluctuations are balanced with the Nusselt solution. The heat exchange with the free surface is enhanced thanks the gravity instability in which liquid recirculation, associated to the convective effects, tends to increase the heat flux across the surface.

4.2. Dynamical system representation

Travelling-wave solutions to (3.12) have been looked after using the `AUTO07p` software [8]. The system of partial differential equations (3.12) simplifies into ordinary differential equations in the moving frame of reference, $\xi = x - c\,t$, where c refers to the phase speed of the waves. The averaged velocity $v = c + q_0/h$ is computed after integration of the mass balance, where $q_0 = \displaystyle\int_0^h (v - c)\,\mathrm{d}y$ is the conserved flow rate in the moving frame. After elimination of v, one is led to a single ODE which is next recast as an autonomous dynamical system in a four-dimensional phase space spanned by $U = (h, \mathrm{d}h/\mathrm{d}\xi, \mathrm{d}^2h/\mathrm{d}\xi^2, \theta)$. Travelling waves correspond to limit cycles in the phase space which arise from Hopf bifurcations of the Nusselt solution $U = (1, 0, 0, \mathcal{B}/[2(1+\mathcal{B})])$. Solitary waves are next found through homoclinic bifurcations by increasing the period of the limit cycles. The procedure is detailed in [13].

We first consider the homoclinic orbits solutions to (3.12) for the set of parameters investigated by [27], *i.e.* $\mathrm{Pr} = 7$, $\widetilde{\mathrm{Bi}} = 0.1$ and $\mathrm{Ka} = 30000$ (see Figure 11 in that

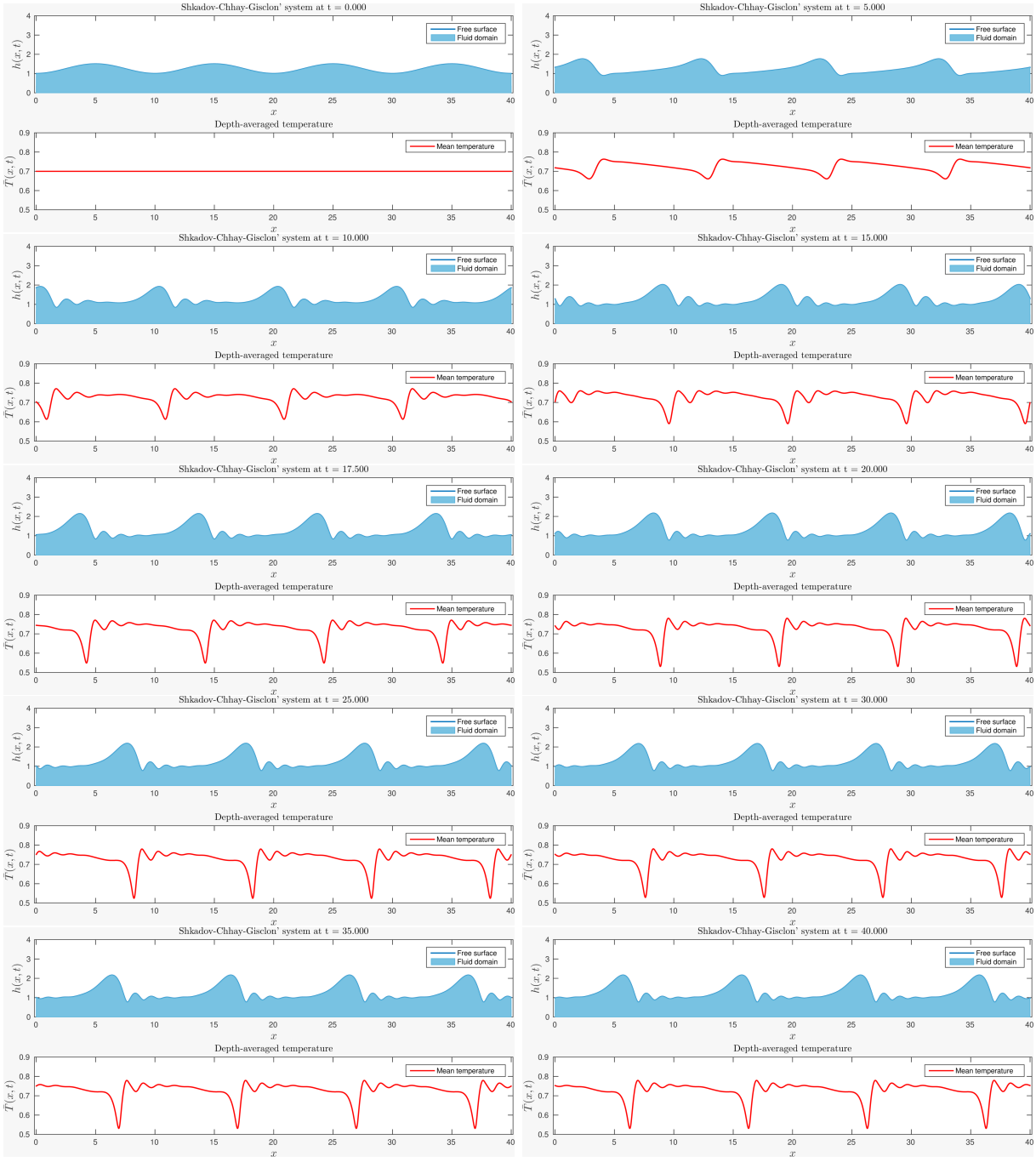

Figure 3. *Time evolution of hydrodynamic free surface and depth-averaged temprature. Parameters are:* $\mathrm{Re} = 1$, $\mathrm{Pe} = 10$, $\mathrm{Bi} = 1$.

reference). These values correspond well to the typical situation of a water film. Figure 4(b) compares the minimum of the temperature at the free surface $T|_{z=h}$ obtained from (3.12) as $T|_{z=h} = 1 - 2\theta$ (dashed lines) with the solution to the Fourier equation (solid lines) and to the averaged energy balance (3.13) (dotted lines). The curves represent a change of

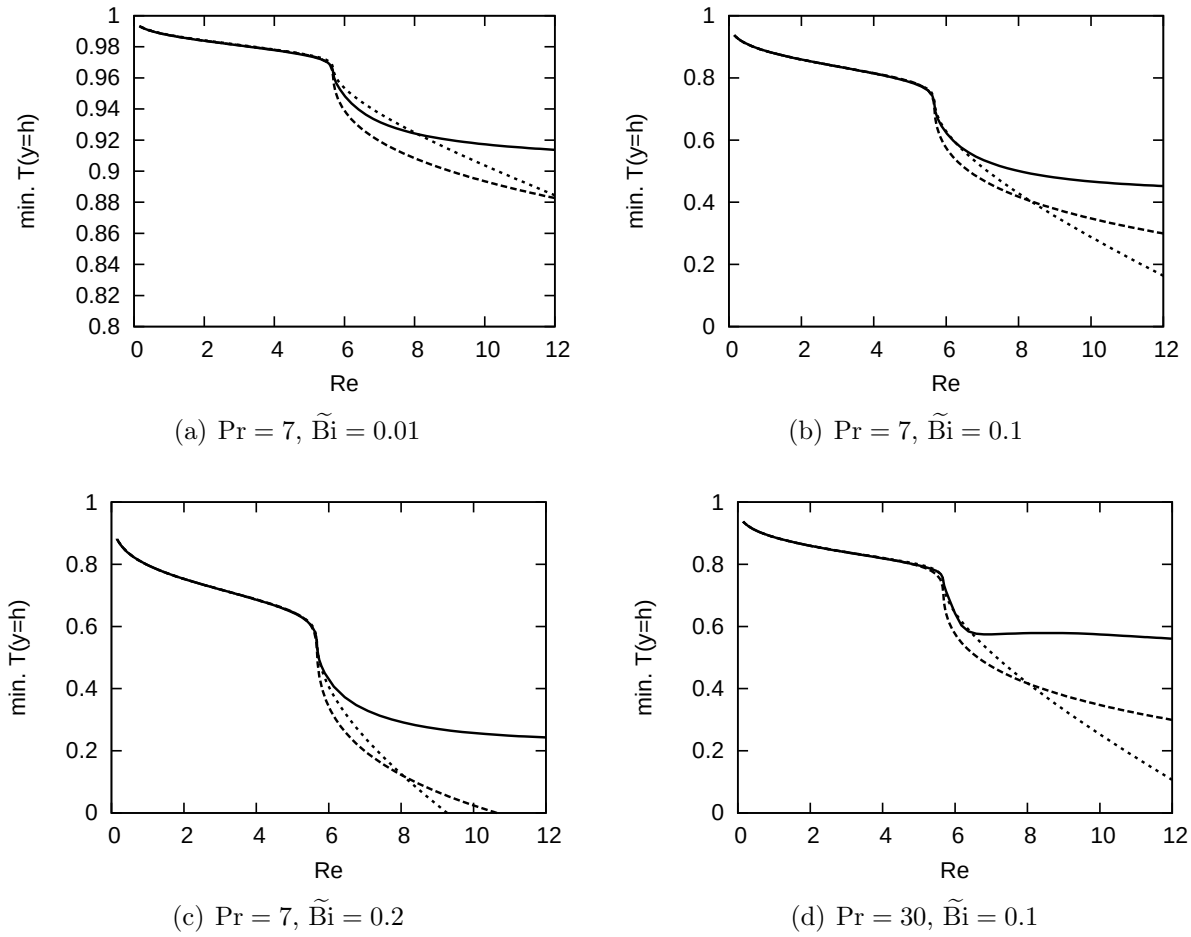

(a) $\mathrm{Pr} = 7$, $\widetilde{\mathrm{Bi}} = 0.01$

(b) $\mathrm{Pr} = 7$, $\widetilde{\mathrm{Bi}} = 0.1$

(c) $\mathrm{Pr} = 7$, $\widetilde{\mathrm{Bi}} = 0.2$

(d) $\mathrm{Pr} = 30$, $\widetilde{\mathrm{Bi}} = 0.1$

Figure 4. *Free surface temperature as function of the Reynolds number for solitary-wave solutions to the Fourier equation (solid lines), to system* (3.12) *(dashed line) and to the averaged energy balance* (3.13) *(dotted line).*

behaviour around $\mathrm{Re} = 6$ which signals the onset of capillary roll-waves in the drag-inertia regime identified by Ooshida [16] where inertia effects become dominant (see [6]). Below this value of the Reynolds number, the curves are very close as a result of the consistency with the long-wave expansion up to first order. Discrepancies are observable whenever inertia effects are significant. They are emphasized when the Prandtl number is raised to $\mathrm{Pe} = 30$ (compare Figures 4(b) and 4(d)). Note that the conservative System (3.12) is closest to the solution of the Fourier equation than the non-conservative equation (3.13). Moreover, at $\mathrm{Pr} = 7$ and $\widetilde{\mathrm{Bi}} = 0.1$, all values of the free surface temperature corresponding to (3.12) fall into the admissible range $[0, 1]$, whereas solutions (3.13) yield non-physical negative values of $T|_{z=h}$. Yet, the conservative system (3.12) is not free from this drawback as raising the Biot number also leads to negative values of $T|_{z=h}$ (*cf.* Figure 4(c)).

5. Conclusions and perspectives

In this article, a new model for heated falling films is proposed: whereas the hydrodynamical part has already been known (see, for example, [5]), the asymptotic model associated to the heat field is derivated in the same formal way. The result corresponds to an explicit conservative model consistent up to the order $\mathcal{O}(\varepsilon)$ with the Fourier–Navier–Stokes equations. The numerical experiments and comparisons with previous works (*e.g.* [27]) and with 2D heat equation direct simulations validate the proposed model.

Thanks to the performed asymptotic development, the resulting model, Equation (3.12), inherits, by derivation, the conservative structure of the celebrated Saint-Venant model. The natural continuation step consists in performing a rigorous mathematical analysis of the proposed model (*e.g.* approximation and asymptotic convergence properties) obtained by formal derivation at this step. From the physical point of view many new effects can be added in future works. For instance, one can mention the mass transfer phenomena across the free surface, viscosity dependence on the temperature and density, *etc.*

Acknowledgments

The authors acknowledge a financial support from CNRS (INSIS, Cellule Énergie, exploratory project call 2014). Moreover, we wish to thank Didier Bresch for helpful discussions on the topic of falling films modeling.

References

[1] T. Benjamin. Wave formation in laminar flow down an inclined plane. *J. Fluid Mech.*, 554(2), 1957. 8

[2] D. J. Benney. Long waves on liquid films. *J. Math. and Phys.*, 45:150–155, 1966. 3

[3] M. Boutounet. *Modèles asymptotiques pour la dynamique d'un film liquide mince*. PhD thesis, Université de Toulouse, 2013. 4

[4] M. Boutounet, L. Chupin, P. Noble, and J.-P. Vila. Shallow water equations for Newtonian fluids over arbitrary topographies. *Comm. Math. Sci.*, 6:29–55, 2008. 8

[5] D. Bresch and P. Noble. Mathematical justification of a shallow water model. *Methods and Applications of Analysis*, 14(2):87–118, 2007. 4, 6, 21

[6] S. Chakraborty, P. K. Nguyen, C. Ruyer-Quil, and V. Bontozoglou. Extreme solitary waves on falling liquid films. *J. Fluid Mech.*, 745:564–591, 2014. 20

[7] S. D'Alessio, J. Pascal, H. Jasmine, and K. Ogden. Film flow over heated wavy inclined surfaces. *J. Fluid Mech.*, 665:418–456, 2010. 10

[8] E. J. Doedel. Auto07p continuation and bifurcation software for ordinary differential equations, 2008. Montreal Concordia University. 17, 18

[9] D. Dutykh, T. Katsaounis, and D. Mitsotakis. Finite volume methods for unidirectional dispersive wave models. *Int. J. Num. Meth. Fluids*, 71:717–736, 2013. 18

[10] E. D. Fernández-Nieto, P. Noble, and J.-P. Vila. Shallow water equations for non-newtonian fluids. *J. Non Newtonian Fluid Mech.*, 165(13-14):712 – 732, 2010. 4

[11] S. W. Joo and S. H. Davis. On the falling film instabilities and wave breaking. *Phys. Fluids*, 3:231–232, 1991. 3

[12] S. W. Joo, S. H. Davis, and S. G. Bankoff. Long-wave instabilities of heated falling films: two-dimensional theory of uniform layers. *J. Fluid Mech.*, 230:117–146, 1991. 3

[13] S. Kalliadasis, C. Ruyer-Quil, B. Scheid, and M. G. Velarde. *Falling liquid films*, volume 176 of *Applied Mathematical Sciences*. Springer, first edition, 2012. 3, 7, 18

[14] P. L. Kapitza. Wave flow of thin layers of a viscous fluid: I. free flow - II. fluid flow in the presence of continuous gas flow and heat transfer. In D. T. Haar, editor, *Collected papers of P. L. Kapitza (1965)*, pages 662–689. Pergamon, 1948. (Original paper in Russian: Zh. Eksp. Teor. Fiz. **18**, I. 3–18, II. 19–28). 3

[15] P. Noble and J. P. Vila. Stability theory for difference approximations of some dispersive shallow water equations and application to thin film flows. *Arxiv:1304.3805*, pages 1–22, 2014. 18

[16] T. Ooshida. Surface equation of falling film flows with moderate reynolds number and large but finite weber number. *Phys. Fluids*, 11:3247–3269, 1999. 20

[17] A. Pumir, P. Manneville, and Y. Pomeau. On solitary waves running down an inclined plane. *J. Fluid Mech.*, 135:27–50, 1983. 3

[18] A. J. Roberts. Low-dimensional models of thin film fluid dynamics. *Phys. Lett. A*, 212:63–71, 1996. 3

[19] V. V. Rusanov. The calculation of the interaction of non-stationary shock waves and obstacles. *USSR Computational Mathematics and Mathematical Physics*, 1(2):304–320, 1962. 18

[20] C. Ruyer-Quil and P. Manneville. Improved modeling of flows down inclined planes. *Eur. Phys. J. B*, 15:357–369, 2000. 3, 4

[21] C. Ruyer-Quil, B. Scheid, S. Kalliadasis, M. G. Velarde, and R. Kh. Zeytounian. Thermocapillary long waves in a liquid film flow. Part 1. Low dimensional formulation. *J. Fluid Mech.*, 538:199–222, 2005. 4, 17

[22] C. Ruyer-Quil, P. Treveleyan, F. Giorgiutti-Dauphiné, C. Duprat, and S. Kalliadasis. Modelling film flows down a fibre. *J. Fluid Mech.*, 603:431–462, 2008. 10

[23] B. Scheid, S. Kalliadasis, C. Ruyer-Quil, and P. Colinet. Interaction of three-dimensional hydrodynamic and thermocapillary instabilities in film flows. *Phys. Rev. E*, 78:066311, 2008. 4

[24] B. Scheid, C. Ruyer-Quil, S. Kalliadasis, M. G. Velarde, and R. Zeytounian. Thermocapillary long waves in a liquid film flow. Part 2. linear stability and nonlinear waves. *J. Fluid Mech.*, 538:223–244, 2005. 4

[25] L. F. Shampine and M. W. Reichelt. The MATLAB ODE Suite. *SIAM Journal on Scientific Computing*, 18:1–22, 1997. 18

[26] V. Ya. Shkadov. Wave flow regimes of a thin layer of viscous fluid subject to gravity. *Izv. Akad. Nauk SSSR, Mekh. Zhidk Gaza*, 1:43–51, 1967. English translation in *Fluid Dynamics* **2**, 29–34, 1970 (Faraday Press, N.Y.). 3

[27] P. Trevelyan, B. Scheid, C. Ruyer-Quil, and S. Kalliadasis. Heated falling films. *J. Fluid Mech.*, 592:295–334, 2007. 4, 17, 18, 21

[28] P. Trevelyan, B. Scheid, C. Ruyer-Quil, and S. Kalliadasis. Heated falling films. *J. Fluid Mech.*, 592:295–334, 2007. 8

LOCIE, UMR 5271 CNRS, Université Savoie Mont Blanc, Campus Scientifique, 73376 Le Bourget-du-Lac Cedex, France
E-mail address: Marx.Chhay@univ-savoie.fr
URL: http://marx.chhay.free.fr/

LAMA, UMR 5127 CNRS, Université Savoie Mont Blanc, Campus Scientifique, 73376 Le Bourget-du-Lac Cedex, France
E-mail address: Denys.Dutykh@univ-savoie.fr
URL: http://www.denys-dutykh.com/

LAMA, UMR 5127 CNRS, Université Savoie Mont Blanc, Campus Scientifique, 73376 Le Bourget-du-Lac Cedex, France
E-mail address: Marguerite.Gisclon@univ-savoie.fr
URL: https://www.lama.univ-savoie.fr/~gisclon/

LOCIE, UMR 5271 CNRS, Université Savoie Mont Blanc, Campus Scientifique, 73376 Le Bourget-du-Lac Cedex, France
E-mail address: Christian.Ruyer-Quil@univ-savoie.fr
URL: https://www.lama.univ-savoie.fr/~gisclon/